Mod Pathol 36 (2023) 100103

MODERN PATHOLOGY

USCAP UNITED STATES AND CANADIAN ACADEMY OF PATHOLOGY
Creating a Better Pathologist

Journal homepage: https://modernpathology.org/

Research Article

Expanding the Molecular Diversity of *CIC*-Rearranged Sarcomas With Novel and Very Rare Partners

Konstantinos Linos[a,*], Josephine K. Dermawan[a], Tejus Bale[a], Marc K. Rosenblum[a], Samuel Singer[b], William Tap[c], Mark A. Dickson[c], Jason L. Hornick[d], Cristina R. Antonescu[a]

[a] *Department of Pathology and Laboratory Medicine, Memorial Sloan Kettering Cancer Center, New York, New York;* [b] *Department of Surgery, Memorial Sloan Kettering Cancer Center, New York, New York;* [c] *Department of Oncology, Memorial Sloan Kettering Cancer Center, New York, New York;* [d] *Department of Pathology, Brigham & Women's Hospital, Harvard Medical School, Boston, Massachusetts*

ARTICLE INFO

Article history:
Received 30 October 2022
Revised 6 January 2023
Accepted 12 January 2023
Available online 21 January 2023

Keywords:
CIC
AXL
CITED1
SYK
LEUTX
undifferentiated round cell sarcoma

ABSTRACT

Capicua transcriptional repressor (*CIC*)-rearranged sarcoma represents a distinct pathologic entity and constitutes the second most prevalent category of undifferentiated round cell sarcomas (URCSs) after Ewing sarcoma. The 2 most common translocations are t(4;19) and t(10;19), resulting in *CIC* fusions with either *DUX4* and DUX4L paralog, respectively; however, other rare variant fusions have also been reported. In this study, we expand the molecular spectrum of *CIC*-gene partners, reporting on 5 cases of URCSs showing *CIC* fusions with *AXL*, *CITED1*, *SYK*, and *LEUTX* by targeted RNA or DNA sequencing. There were 4 female patients and 1 male patient with a wide age range (12-70 years; median, 36 years). Four cases occurred in the deep soft tissues (lower extremity, 3; neck, 1) and 1 case in the central nervous system (midbrain/thalamus). All cases showed similar histologic findings within the spectrum of URCSs. Immunohistochemistry, showed variable positivity for ETV4 in 4 of the 4 cases and positive results for ERG in 3 of the 4 cases and for WT1 in 1 of the 4 cases. CD31 showed positivity in 2 of the 3 cases, including one coexpressing ERG. Unsupervised clustering of methylation profiles by T-distributed stochastic neighborhood embedding performed in 4 cases showed that all clustered tightly together and along the *CIC* sarcoma methylation class. RNA-sequencing data showed consistent upregulation of *ETV1* and *ETV4* mRNA in all cases examined, at similar levels to *CIC::DUX4* URCSs. Our study expands the molecular diversity of *CIC*-rearranged URCSs to include novel and rare partners, providing morphologic, immunohistochemical, gene expression, and methylation evidence supporting their classification within the family of tumors harboring the more common *DUX4*/*DUX4L* partner genes.

Introduction

Capicua transcriptional repressor (*CIC*)-rearranged sarcomas constitute the second most common category of undifferentiated round cell sarcomas (URCSs), being a distinct pathologic entity with a worse prognosis than Ewing sarcoma (ES) and less responsive to chemotherapy.[1] The most common fusions result from either t(4;19) or t(10;19) translocations, where *CIC* is fused to either *DUX4* or *DUX4L* paralog, respectively,[2,3] although other rare gene partners (*FOXO4*, *NUTM1*, and *NUTM2A*) have also been reported.[1,4-7]

CIC protein is a high-mobility group (HMG) box transcription repressor that binds to target promoters and enhancers. Its default inhibitory activity relies on suppressing transcription in the absence

* Corresponding author.
E-mail address: linosk@mskcc.org (K. Linos).

0893-3952/$ - see front matter
https://doi.org/10.1016/j.modpat.2023.100103

of signaling, whereas its phosphorylation prevents its nuclear import and attenuates its DNA-binding activity.[8-11] The CIC-fusion oncoprotein is a potent transcriptional activator that binds and upregulates the promoters of downstream targets, such as polyoma enhancer activator 3 (PEA3) subfamily of genes (including ETV1/4/5), at both the mRNA and protein levels.[12-14] This gene expression signature is highly pathognomonic and quite specific for diagnostic purposes among URCSs; the latter being especially important as both RNA sequencing and fluorescence in situ hybridization (FISH) have low sensitivity in this setting and may produce false-negative results.[15,16] Consequently, ETV4 immunohistochemistry and RNA in situ hybridization of ETV1/4/5 have been reported to be useful ancillary studies in supporting the diagnosis.[17,18] Gene expression profiling has also shown upregulation of *WT1*, which can be exploited immunohistochemically with similar sensitivity, albeit inferior specificity, to ETV4.[13,17] Unsupervised hierarchical clustering of RNA sequencing showed that *CIC*-rearranged sarcomas cluster into a distinct group separate from other small round blue cell tumors.[15]

In this study, we report 5 cases of *CIC*-rearranged URCSs with novel and very rare gene partners expanding on their molecular diversity. We provide morphologic, immunohistochemical, and molecular support that they are similar to their more common *CIC::DUX4* counterparts.

Materials and Methods

Study Cohort

After approval from the institutional review board of Memorial Sloan Kettering Cancer Center, *CIC*-rearranged URCS were identified from the files of the Department of Pathology, Memorial Sloan Kettering Cancer Center, and the personal consultation files of the senior author (C.R.A). Thus, 5 cases with novel and rare partners were identified and included in this study. Clinical data, such as age, sex, anatomic site, treatment, and follow-up, were retrieved from pathology reports and clinical records. Hematoxylin-and-eosin–stained slides and immunohistochemical stains from all specimens were reviewed by 2 of the authors (K.L., C.R.A).

Immunohistochemistry

The relevant antibodies and dilutions used in this study can be seen in Supplementary Table S1.

Fluorescence In Situ hybridization

FISH analysis was performed on interphase nuclei of paraffin-embedded 4-mm sections using bacterial artificial chromosome clone, flanking *CIC* in 19q13.[1,3] Two hundred tumor nuclei were evaluated using a Zeiss fluorescence microscope (Zeiss Axioplan), controlled by Isis 5 software (Metasystems). A cutoff of >20% nuclei showing a break-apart signal was considered to be a positive result for rearrangement. Nuclei with an incomplete set of signals were omitted from scoring.

Targeted RNA Sequencing (MSK-Fusion)

Detailed descriptions of MSK-Fusion, an amplicon-based targeted RNA next-generation sequencing (NGS) assay using the Archer FusionPlex standard protocol, were described previously.[19] In brief, RNA was extracted from formalin-fixed paraffin-embedded tumor materials, followed by cDNA synthesis. cDNA libraries were prepared using the Archer FusionPlex standard protocol. Fusion unidirectional GSPs have been designed to target specific exons in 123 genes known to be involved in chromosomal rearrangements based on current literature. The final targeted amplicons were ready for 2 × 150-bp sequencing on an Illumina MiSeq sequencer. FASTQ files were automatically generated using the MiSeq reporter software (version 2.6.2.3) and analyzed using the Archer analysis software (version 5.0.4). Each fusion call was supported by a minimum of 5 unique reads and a minimum of 3 reads with unique start sites. Archer FusionPlex was performed in 4 cases.

RNA expression values for Archer probes targeting *ETV1* and *ETV4* for *CIC*-rearranged samples (n = 5) and control clinical samples consisting of various small round blue cell tumors (n = 7; ES, *BCOR*-rearranged sarcoma, desmoplastic small round cell tumor, myxoid/round cell liposarcoma, or *EWSR1*::*NFATC2* sarcoma) were downloaded from the Archer data portal. The expression levels were arbitrary values normalized to the average expression of Archer's internal control. Heatmap was generated by the pHeatmap package (version 1.0.12) using the R software (version 4.1.0).

Targeted DNA Sequencing (MSK-IMPACT Solid)

Detailed descriptions of MSK-IMPACT workflow and data analysis, a hybridization capture-based targeted DNA NGS assay for solid tumors, have been described previously in detail.[20] MSK-IMPACT Solid was performed in all 5 cases.

Methylation Profiling and Clustering Analysis

Four *CIC*-rearranged tumors with novel and rare partners were tested by methylation profiling. Details on methylation profiling have been published previously.[21] In brief, genomic DNA was extracted from formalin-fixed paraffin-embedded tissue sections for each of the samples. Next, 250 ng of genomic DNA was subjected to bisulfite conversion and processed on the Illumina methylation EPIC/850k platform according to the manufacturer's instructions.

We used several external, publicly available data sets to enhance the analysis. First, we obtained raw IDAT files for 148 samples from the Heidelberg sarcoma methylation classifier reference cohort (Gene Expression Omnibus study accession number GSE140668)[22]: 36 alveolar rhabdomyosarcomas, 30 embryonal rhabdomyosarcomas, 26 desmoplastic small round cell tumors, 37 ES, 11 *CIC*-rearranged round cell sarcomas, and 8 *BCOR*-altered round cell sarcomas.

IDAT processing and data analysis on all 152 samples was performed using the R software (version 4.1.0) and the "minfi" package (version 1.38.0).[23] Normalization was performed using the preprocess Illumina function, and probes with a detection *P* value of >.01 were filtered as were single-nucleotide polymorphism–related probes and probes on sex chromosomes. Methylation levels were measured using β values for all cases.[24]

For unsupervised clustering, dimensionality reduction was performed by the T-distributed stochastic neighborhood embedding (t-SNE) method. After normalizing the input data matrix (centering the mean of each column to zero), the top 10,000 most variable CpGs by variance were analyzed using the "Rtsne"

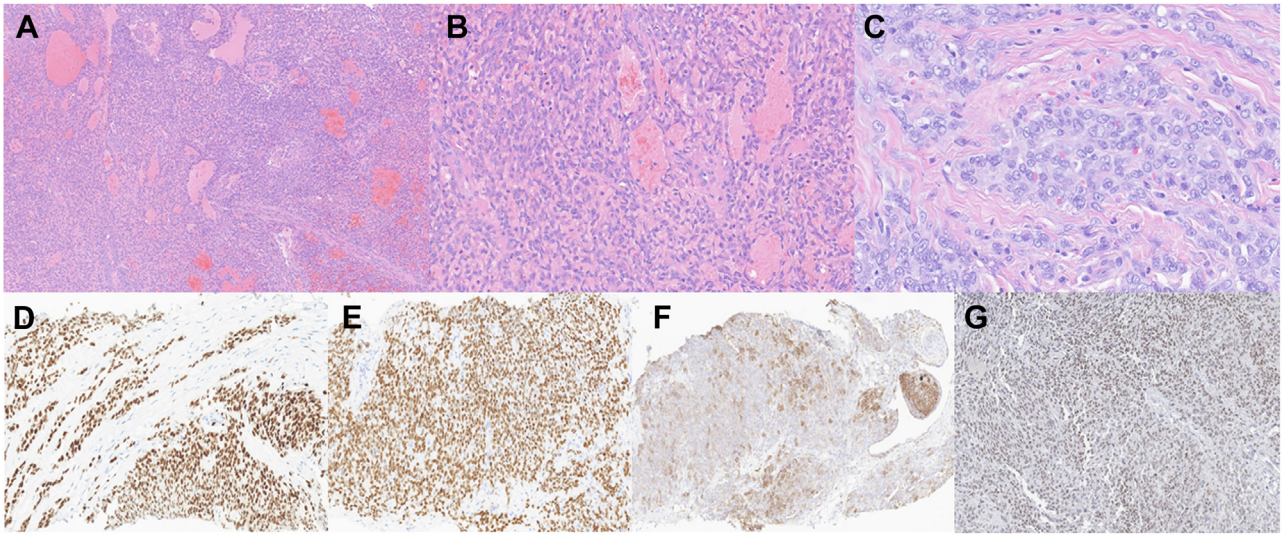

Figure 1.
Morphologic and immunohistochemical findings of case 1 (*CIC::AXL*). (A-C) Sections show sheets of round to spindle cells without any obvious line of differentiation. Pseudovascular spaces lined by neoplastic cells are evident. On higher magnification, the cells exhibit high nuclear-to-cytoplasmic ratio with vesicular chromatin pattern and inconspicuous nucleoli (×50, ×200, ×400). ERG (D) and WT1 (E) show diffuse strong nuclear positivity. (F) CD99 shows patchy membranous expression. (G) ETV4 shows diffuse weak-to-moderate nuclear positivity.

package (version 0.15) with the following nondefault parameters: perplexity = 10, max_iter = 5000, and θ = 0.

Results

Clinical and Histopathologic Findings

The cohort comprised 4 female patients and 1 male patient, all except 1 tumor occurring in adults, with an age range of 12 to 70 years (median, 36 years; mean, 37.8 years) (Figs. 1-4 and Table 1). Four tumors involved the deep soft tissues (the neck, foot, buttock, and lower extremity), and 1 occurred in the central nervous system (CNS; midbrain/thalamic). The tumor sizes ranged from 3.0 to 11.5 cm (median, 4.6 cm; mean, 5.9 cm) in the greatest dimension. All 5 patients presented with primary tumors at diagnosis. All tumors showed similar histologic findings within the spectrum of URCS. They were composed of solid sheets and nests of round to ovoid to epithelioid cells with a high nuclear-to-cytoplasmic ratio, amphophilic to clear cytoplasm, vesicular chromatin pattern, and mild to moderately conspicuous nucleoli. One tumor showed a minor spindle cell component and a focal pseudoalveolar pattern. In 1 case, a more prominent myxoid matrix was evident, in which the cells were arranged in a reticular or trabecular fashion. In the CNS tumor, the cells were variably discohesive with a pattern of growth ranging from nests to sheet-like to papillary. In some cells, apparent fibrillary and/or refractile cytoplasmic inclusions were observed, whereas occasionally multinucleation was also noted. These 2 tumors were multilobulated with interlobular fibrous bands. The mitotic figures ranged from 8 to 35 per 1.0 mm^2. Two patients had resections of their primary tumors postneoadjuvant therapy, whereas 1 patient had a primary resection without neoadjuvant therapy. One patient presented with a recurrence near the stump of below-the-knee amputation 6 months before. Subsequent above-the-knee amputation was performed postneoadjuvant therapy. Necrosis was present in the pretreatment specimens of cases 2 and 5; in their posttreatment resections, 30% to 40% necrosis and fibrosis and 30% necrosis, respectively, were evident. In case 1, there was no histologic treatment effect postneoadjuvant resection; however, the tumor was reduced in size from 5.1 to 3.2 cm in the greatest dimension. The surgical margin was positive in 1 of the 4 of the cases (case 3, primary resection without neoadjuvant treatment).

Immunohistochemical Findings

ETV4 was evaluated in 4 tumors and showed diffuse positivity with weak-to-moderate intensity in 2 (*CIC::AXL* and *CIC::CITED1*) and focal (<5% of tumor volume) weak-to-moderate expression in the other 2 (*CIC::LEUTX* and *CIC::SYK*) (Figs. 1-4 and Table 1). ERG was positive in 3 of the 4 cases evaluated, whereas WT1 showed diffuse nuclear positivity in 1 tumor and it was essentially negative in the other 3 cases examined. CD31 staining showed positive results in 2 of the 3 cases; it was coexpressed with ERG in 1 case, whereas in the other case, ERG was negative. CD99 showed nonspecific positivity in 3 of the 3 tumors evaluated (patchy cytoplasmic in 2 and paranuclear dot-like pattern in 1). CAM5.2 showed rare positive cells in 1 of the 2 cases, whereas EMA and SMA showed focally and weakly positive results in 1 of the 3 and 1 of the 2 cases, respectively. Vimentin and TLE1 (patchy) exhibited positive results in 1 case tested. Nuclear expression of SMARCB1 (BAF-47, INI1) was retained in 3 of the 3 cases, and SMARCA4 (BRG1) was retained in 1 case tested. The following immunohistochemical stains showed negative results in the cases evaluated: S100, desmin, myogenin, MyoD1, CKMNF116, CD34, CD45, ALK, Pan-Trk, SS18-SSX, PanCK, CK7, CK20, EMA, BCOR, SATB2, TdT, HMB45, MelanA, CD163, p63, calponin, GFAP, AFP, inhibin, CD10, TTF-1, PAX-8, OCT-4, PR, chromogranin, synaptophysin, and neurofilament protein.

Fluorescence In Situ Hybridization

In case 1 with *CIC::AXL* fusion, the initial FISH showed loss of the 5' portion of the *CIC* locus in 93% of cells, indicative of a *CIC*

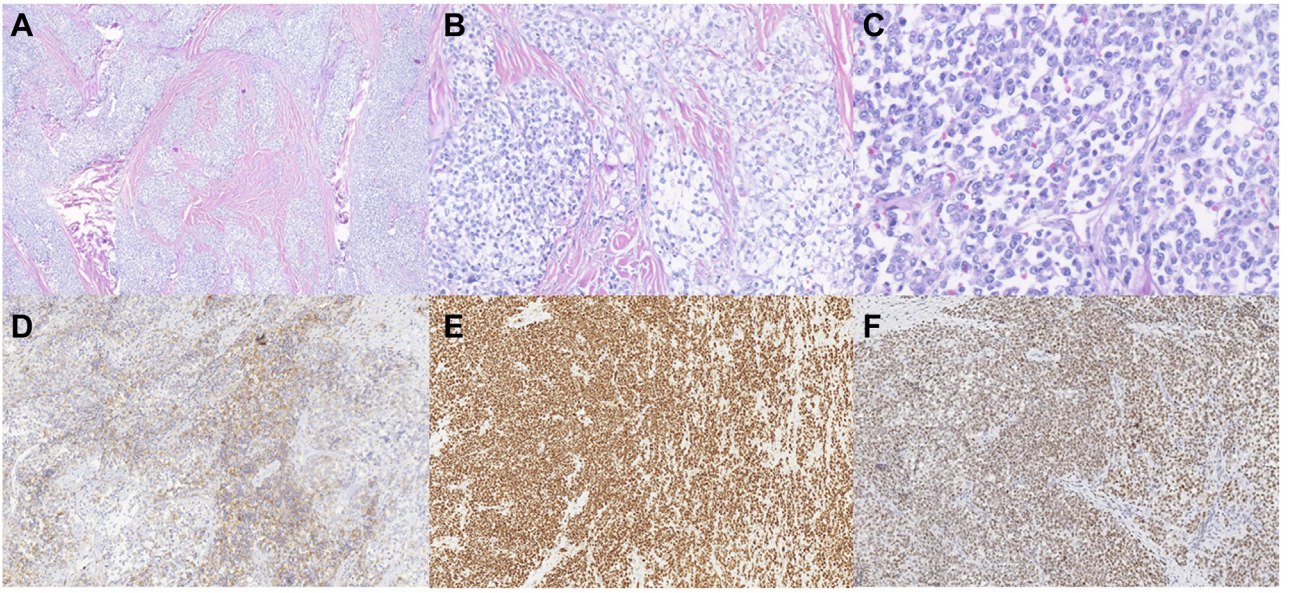

Figure 2.
Morphologic and immunohistochemical findings of case 2 (*CIC::CITED1*). (A-C) Low-power magnification shows a multinodular growth pattern in a collagenous background. Medium- and high-power magnifications show epithelioid cells with minimal eosinophilic to clear cytoplasm and vesicular chromatin pattern with mildly conspicuous nucleoli (×50, ×100, ×400). (D) Immunohistochemistry for CD99 shows patchy positivity. Diffuse positivity for ERG (E) and ETV4 (F).

fusion (Table 2). In 2 cases, the FISH analysis showed negative results for *EWSR1* rearrangement and, in another case, for *FUS* and *SS18* gene rearrangements.

Targeted RNA-Sequencing Results (Archer FusionPlex)

Archer FusionPlex was performed in 4 tumors, which detected in-frame fusions between genes *CIC* exon 20 (NM_015125) and *AXL* exon 2 (NM_001699) (case 1); *CIC* exon 20 (NM_015125) and *CITED1* exon 3 (NM_004143) (case 2); and *CIC* exon 20 (NM_015125) and *LEUTX* exon 3 (NM_001143832) (case 4) (Fig. 5 and Table 2). Archer FusionPlex showed negative results for gene fusions in case 5, whereas it was not performed in case 3.

Targeted DNA Sequencing Results (MSK-IMPACT Solid)

In case 3, a *CIC* (NM_015125)::*LEUTX* (NM_001143832) fusion—c.4797:CIC c.354:LEUTXdup, was detected, resulting in

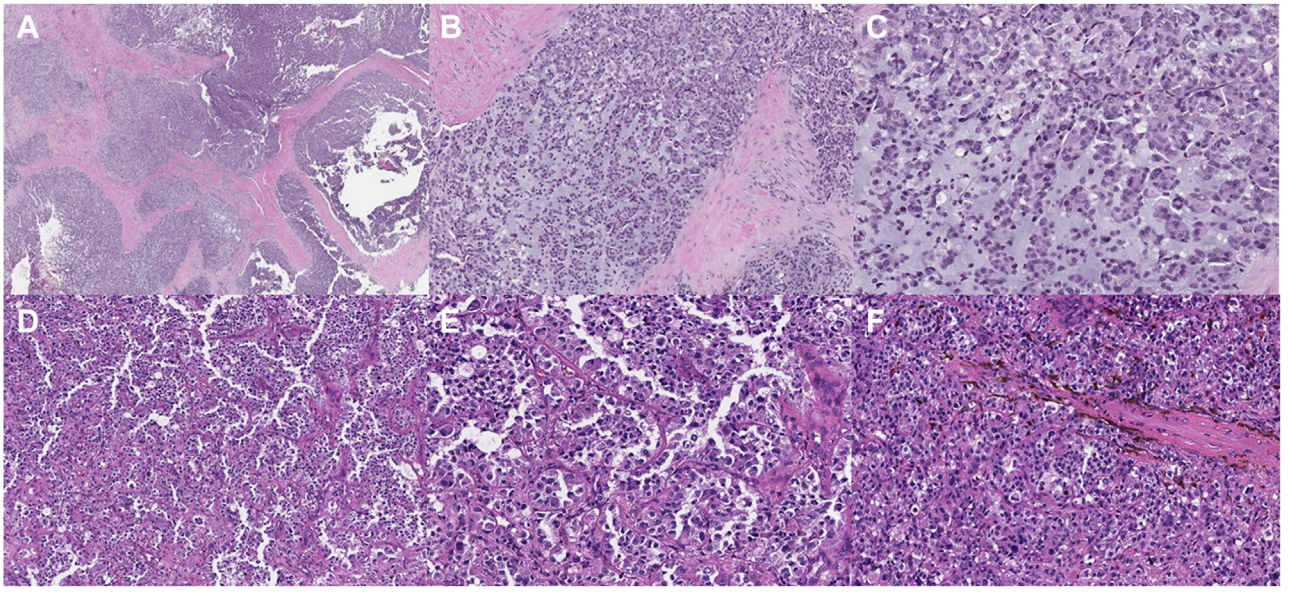

Figure 3.
Morphologic findings of cases 3 and 4 (*CIC::LEUTX*). (A-C) Low-power magnification shows a multinodular growth pattern, whereas medium- and high-power magnifications show epithelioid cells with eosinophilic cytoplasm in a myxoid background (×50, ×100, ×200). (D-F) This primary CNS tumor shows dyshesive epithelioid cells in a pseudoalveolar pattern, whereas, in other areas, there is a more solid growth pattern. Cells show ample eosinophilic cytoplasm with nuclear pleomorphism (×100, ×200).

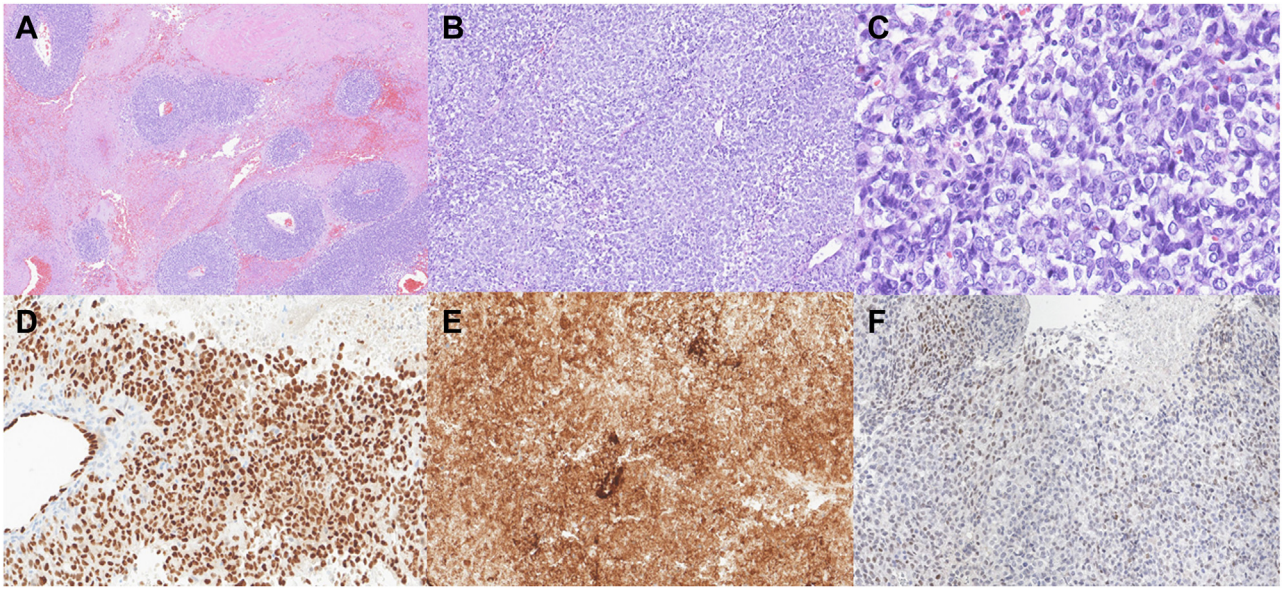

Figure 4.
Morphologic and immunohistochemical findings of case 5 (*CIC::SYK*). (A) Sections show large areas of necrosis with perivascular accentuation of viable tumor (×50).) Medium- (B) and high-power (C) magnifications show a proliferation of round to vaguely spindle cells with no obvious line of differentiation morphologically. The cells exhibit vesicular chromatin pattern with inconspicuous nucleoli (×100, ×400). (D) Diffuse nuclear expression of ERG. Note the internal positive control of background endothelial cells with no expression in the surrounding pericytes. (E) Diffuse membranous and cytoplasmic expression of CD31. (F) ETV4 shows focal weak immunoreactivity.

the fusion of *CIC* exons 1-20 to a part of *LEUTX* exon 3 (Fig. 5 and Table 2). In cases 1, 2, and 4, MSK IMPACT was able to confirm the gene fusions detected at the RNA level by Archer FusionPlex. Moreover, in case 2, MSK IMPACT detected the same fusion in the brain metastasis. In case 5, in which Archer FusionPlex showed negative results, MSK-IMPACT detected a *CIC* (NM_015125) rearrangement with a breakpoint in exon 20: t(9;19)(q22.2;q13.2) (chr9:g.93665094::chr19:g.42799213), with the breakpoint on chr9 being 2.3 kilobases downstream of the nearest coding gene (*SYK*).

In case 1, the *CIC::AXL* rearrangement was a duplication that resulted in a fusion of *CIC* exon 1-20 to *AXL* exons 2-20, including the kinase domain of *AXL*. The somatic alteration *FAT1* (NM_005245) exon 10 p.L1625 *(c.4874T>G) was also detected,

Table 1
Clinical and pathologic features

Case	Age/sex	Location	Tumor size (cm)	Pertinent IHC	Chemotherapy/radiation treatment	Surgical treatment, margins	Histologic treatment response	Follow-up (mo)
1	29/F	Left lower neck	5.1	ERG^{+}, WT-1^{+}, CD99^{+} (patchy), ETV4^{+}[a] CD31^{-}	Neoadjuvant VAC/IE[b]	Resection, negative margins	No treatment response[c]	NED (2)
2	36/F	Right foot	4.2	ERG^{+}, WT-1^{-}, CD99^{+} (patchy), ETV4^{+}[d] CD31^{-}	Neoadjuvant VAC/IE, adjuvant temozolomide, and irinotecan	Resection, negative margins	30%-40% in the form of fibrosis and necrosis	AWD (lung and brain metastases) (19)
3	12/F	Left buttock	3.0	WT-1^{-}, CD99 (paranuclear dot-like), CD31^{-}	Adjuvant radiation to the primary site (55.8 Gy), ifosfamide with doxorubicin or etoposide for lung metastases, whole lung radiation (15 Gy)	Primary excision, positive margins	NA	NED (108)
4	42/F	Midbrain/ thalamus	NA	ERG^{-}, WT1^{-}, CD31^{+} (strong), ETV4$^{+/-}$[e]	Neoadjuvant brain radiation therapy and temozolomide	No surgical treatment	NA	NED (51)
5	70/M	Lower extremity	11.5	ERG^{+}, CD31^{+} (strong), ETV4$^{+/-}$[f]	Doxorubicin, paclitaxel plus nivolumab for local recurrence and lung metastasis, gemcitabine and docetaxel postlocal recurrence resection	Resection of local recurrence, negative margins	30% necrosis	NED (12)

AWD, alive with disease; CNS, central nervous system; IHC, immunohistochemistry; NA, not available; NED; no evidence of disease; VAC/IE, vincristine, doxorubicin, and cyclophosphamide/ifosfamide and etoposide.
[a] Diffuse weak to focally moderate, +.
[b] Vincristine, doxorubicin, and cyclophosphamide alternating with ifosfamide and etoposide.
[c] No treatment response histologically but tumor reduced in size from 5.1 to 3.2 cm in the greatest dimension.
[d] Diffuse moderate, +.
[e] Focal moderate, + (<5% tumor volume).
[f] Focal weak, + (<5% tumor volume).

Table 2
FISH and RNA and DNA sequencing results

Case	RNA sequencing (Archer FusionPlex)	DNA sequencing (MSK IMPACT); FISH
1	In-frame *CIC* exon 20::*AXL* exon 2 with a 2-bp insertion	*CIC::AXL*: c.4663:*CIC*_c.151:*AXL*dup; loss of 5 portion of *CIC* locus, indicative of fusion
2	In-frame *CIC* exon 20::*CITED1* exon 3	*CIC::CITED1:* t(19;X)(q13.2;q13.1)[a]; negative for *EWSR1*, *FUS*, and *SS18* rearrangements
3	Not done	*CIC::LEUTX*: c.4797:CIC_c.354:*LEUTX*dup; negative for *EWSR1* rearrangement
4	In-frame *CIC* exon 20::*LEUTX* exon 3	*CIC::LEUTX*: c.4769:CIC_c.321:*LEUTX*dup; none
5	Negative	*CIC* breakpoint in exon 20: t(9;19)(q22.2;q13.2)[b]; none

FISH, fluorescence in situ hybridization
[a] The same fusion was detected in the primary tumor and brain metastasis.
[b] The nearest gene on chr9 where the breakpoint occurred is *SYK*.

whereas the copy number profile was suggestive of broad copy number gain on chromosome 12 and broad copy number loss of chromosome arms 16q23.24 and 19p13.

Additional copy number changes in the remaining cases were broad copy number gains on chromosome 8 and broad copy number losses of chromosome arms 9q, 11q22-23, and 17q11-17q21. The estimated tumor mutation burden of the entire cohort ranged from 0.8 to 1.6 mutations per megabase. All tumors were microsatellite stable (MSIsensor score ranged from 0.12 to 0.76).[25] The somatic alterations and copy number changes of all cases are summarized in Supplementary Table S2.

Unsupervised t-distributed stochastic neighborhood embedding Clustering of Methylation Profiles and Sarcoma Methylation Classifier

Unsupervised clustering of methylation profiles by t-SNE showed that the 4 cases (*AXL*, *LEUTX* [case 4], *CITED1*, and *SYK*) clustered tightly together with the *CIC* sarcoma methylation class, as described by Koelsche et al,[22] and were distinct from other small round blue cell tumors (alveolar rhabdomyosarcoma, embryonal rhabdomyosarcoma, desmoplastic small round cell tumor, ES, and *BCOR*-rearranged sarcomas) (Fig. 6).

Upregulation of ETV1/4 mRNA

Targeted RNA sequencing data showed that the *CIC::AXL*, *CIC::CITED1*, and *CIC::SYK* cases exhibited consistent upregulation of *ETV1* and *ETV4* mRNA at various levels (Fig. 7); this was similar to *CIC::DUX4* URCS and in contrast to other round cell/undifferentiated sarcoma controls with various fusions, which expressed near-zero levels.

Treatment and Follow-Up

Two patients (cases 1 and 2) received neoadjuvant chemotherapy with vincristine, doxorubicin, and cyclophosphamide/ifosfamide and etoposide. One patient (case 2) received temozolomide and irinotecan, palliative brain radiation, and gemcitabine with docetaxel for metastatic disease (Table 1). One patient (case 3) received ifosfamide with doxorubicin or etoposide for lung metastases with near obliteration of distant disease, followed by localized adjuvant radiation to the primary site (55.8 Gy) and whole lung radiation (15Gy). One patient (case 4) received neoadjuvant brain radiation with subsequent temozolomide, and one patient (case 5) received doxorubicin, followed by paclitaxel and nivolumab, as part of a clinical trial for local recurrence and possible metastases.

The follow-up ranged from 2 to 108 months (median, 19 months; mean, 38.4 months). Overall, 1 patient developed lung and brain metastases, 1 patient solely lung metastases, and 1 patient local recurrence at the stump of previous below-the-knee amputation and lung metastases. Three patients were alive with no evidence of disease, 1 patient was alive with localized disease, and 1 patient was alive with distant disease.

Discussion

This study reports 5 new cases of *CIC*-rearranged URCSs with novel and very rare fusion partners (*AXL*, *CITED1*, *LEUTX*, and *SYK*).

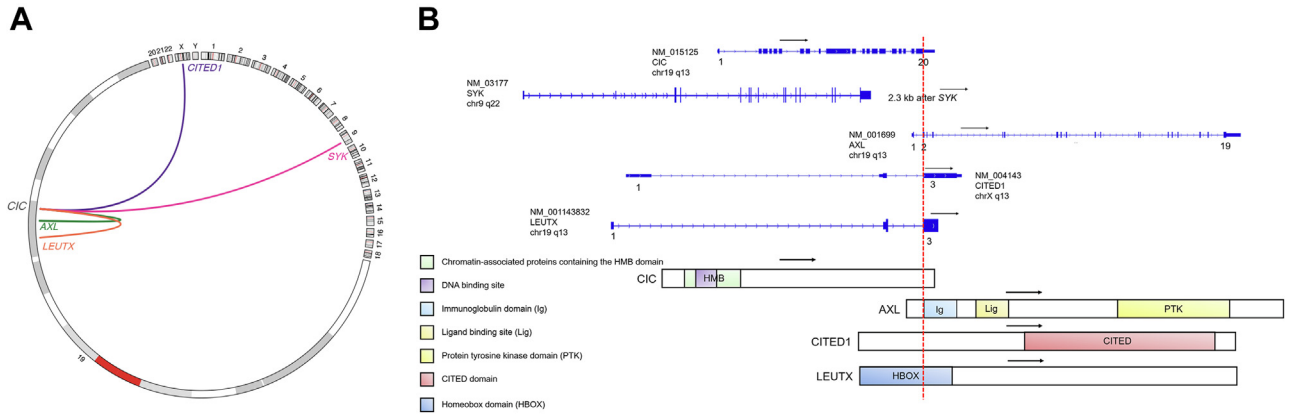

Figure 5.
(A) Circos plot depicting *CIC* fusions represented by links between cytobands (hg19 genome). Plot generated using R package "circlicize," version 0.4.13. (B) Schematics of *CIC* fusion transcripts annotated by NCBI RefSeq accession numbers and the predicted chimeric protein domains. Numbers, black arrows, and red dotted lines represent exons, directions of transcript, and fusion breakpoint, respectively.

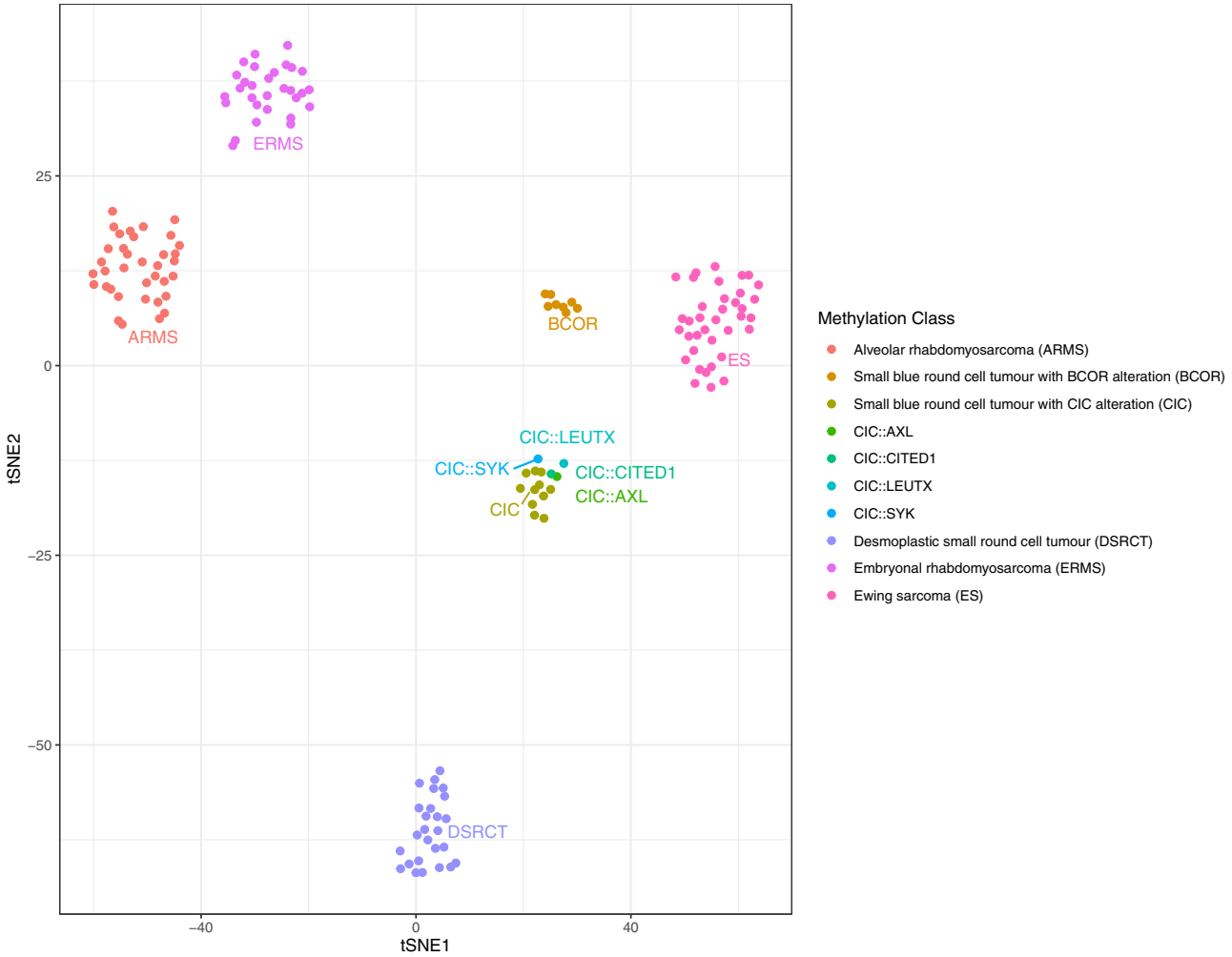

Figure 6.
Unsupervised clustering of methylation profiles by t-SNE showed that the 4 cases (*AXL*, *LEUTX* [case 4], *CITED1*, and *SYK*) clustered tightly together with the *CIC* sarcoma methylation class and were distinct from other small round blue cell tumors (alveolar rhabdomyosarcoma, embryonal rhabdomyosarcoma, desmoplastic small round cell tumor, Ewing sarcoma, and *BCOR*-rearranged sarcomas).

In contrast to *CIC::DUX4* sarcomas in which there is a slight male dominance, in this cohort, there was a female predominance (M/F: 1:4), whereas the mean age at diagnosis (37.8 years) was slightly older. In all cases, the morphologic features were those of an undifferentiated sarcoma within the spectrum of what has been described in *CIC*-rearranged sarcomas.[1] Moreover, similar to cases harboring the canonical fusion, the immunohistochemical profile of this study group also showed an expression of ETV4, ERG, and WT1 with variable positivity. In all cases, the breakpoints were within exon 20 of *CIC*, similar to the most reported cases harboring *CIC::DUX4*, *CIC::FOXO4*, and *CIC::LEUTX* fusions, with retention of the HMG box DNA-binding domain.[3,11,26] *NUTM1*, albeit still very rare, seems to be the second most common partner in *CIC*-rearranged undifferentiated sarcomas with otherwise typical morphology.[27] In contrast to the tumors presented in our cohort, these tumors have a predisposition to the axial location with frequent bone involvement.[7,27,28] Although initially considered predominant in childhood, it seems that they have a broader age distribution closer to that of *CIC::DUX4* undifferentiated sarcomas. Breakpoints within exons 16 to 20 of *CIC* with retention of the HMG box DNA-binding domain have been documented as well. In case 2, a broad copy number gain of chromosome 8 was detected, which is a common recurrent abnormality in *CIC::DUX4* sarcomas and has been reported in undifferentiated sarcomas with *CIC-NUTM1* fusion.[27,29] In the 3 cases with postneoadjuvant therapy resection, the treatment response was poor (up to 40%, grade I response), similar to other *CIC*-rearranged sarcomas.[1] However, the patient with a primary CNS tumor (case 4) showed no post-treatment evidence of disease radiologically, and in cases 3 and 5, the lung metastases were not detectable after radiation and chemotherapy. In contrast to patients with *CIC::DUX4* or *CIC::-NUTM1* sarcomas who experience a poor 5-year survival, all patients in our cohort were alive, albeit with a limited median follow-up of 19 months. Nevertheless, the number of subjects in this study is admittedly too low to draw meaningful statistical conclusions.

AXL is a member of the TAM family of tyrosine kinase receptors (Tyro-3, AXL, and MER).[30] Ligand binding to the extracellular domain usually leads to its activation by dimerization and trans-autophosphorylation of tyrosine residues.[30] In adult tissues, it is expressed ubiquitously mediating a diverse array of cellular functions; in neoplasia, it has been implicated in the development and progression of many malignancies by playing a role in cancer cell proliferation, migration, and invasion, angiogenesis, and

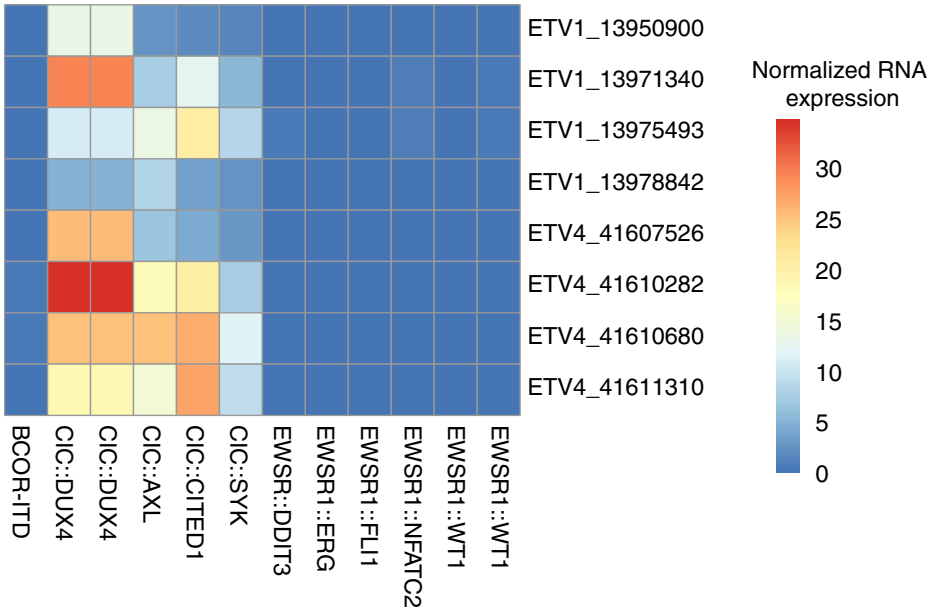

Figure 7.
Heatmap depicting RNA expression values for Archer probes targeting ETV1 and ETV4 for *CIC*-rearranged samples and control clinical samples consisting of various small round blue cell tumors (Ewing sarcoma, *BCOR*-rearranged sarcoma, desmoplastic small round cell tumor, myxoid/round cell liposarcoma, and *EWSR1::NFATC2* sarcoma). Row names denote gene symbols and chromosomal start coordinates of probe targets. Column names denote underlying gene fusions of the corresponding sample. Expression levels were normalized to average expression of each probe of Archer internal control.

metastasis.[30] In case 1, exon 20 of *CIC* was fused with exon 2 of *AXL*, expected to encode for the entire protein kinase domain of *AXL*, presumably leading to activation of *CIC* by phosphorylation.

CITED1 (CREB-binding protein/P300 interacting transactivator with glutamic acid [E]/aspartic acid [D]-rich carboxy-terminal domain 1) is located on chromosome Xq13.1 and belongs to the CITED family of nuclear proteins (CITED1-4), which coregulate transcriptional nuclear proteins through the transactivation domain.[31] In mesenchymal neoplasia, CITED1 has been described in *SRF*-fused perivascular tumors (*SRF::CITED1*), whereas CITED2 has been reported in spindle cell rhabdomyosarcoma (*VGLL2::CITED2*) and *PRDM10*-rearranged soft tissue tumors (*PRDM10::CITED2*).[31-33] Only 1 case of URCS with an in-frame *CIC::CITED1* has been published in the literature.[34] The breakpoints were between exon 21 of *CIC* and exons 4 and 5 of *CITED1*. The patient received chemotherapy, ponatinib, and pazopanib and eventually died of disease.

LEUTX gene is a paired homeobox gene located at chromosome 19q13, which belongs to the same class as *DUX4*.[35] It plays an important role in embryonal development, and its expression is mostly suppressed postnatally.[36] Fusions of *LEUTX* have been described in a case of malignant epithelioid peripheral nerve sheath tumor (*BRD4::LEUTX*) and a case of therapy-related acute myeloid leukemia (*KAT6A::LEUTX*).[37,38] To this date, *CIC::LEUTX* has been described in 6 cases (2 angiosarcomas [soft tissue and CNS], 1 intraspinal extramedullary subdural URCS, 1 anaplastic ganglioglioma, 1 anaplastic astrocytoma, and 1 CNS embryonal tumor).[11,36,39-41] One of our cases represents the first extra-CNS case of URCS with this fusion. In both of our cases, the breakpoints were between *CIC* exon 20 and *LEUTX* exon 3, which are identical with the 4 of the 6 reported *CIC::LEUTX* cases in which information regarding breakpoints is known. Intriguingly, 2 of the 6 *CIC::LEUTX* reported (1 CNS angiosarcoma and 1 embryonal tumor) harbored *TSC2* somatic mutations similar to our CNS case[39,41] (Supplementary Table S2); it is unknown if the other cases also harbored *TSC2* mutations because they were not reported. In the CNS embryonal tumor, the detected somatic *TSC2* variant c.G2714A was evaluated as pathogenic mutation by public database ClinVar. The patient received chemotherapy and radiotherapy along with mTOR inhibitor (everolimus) with significant clinical response.[39] Nevertheless, in our cohort, the detected *TSC2* mutation in case 4 (c.3889G>A p.A1297T) (supplementary Table S2) is predicted to be benign or likely neutral in ClinVar.

The *SYK* gene (spleen tyrosinase kinase), located on 9q22, encodes for a member of the family of nonreceptor type Tyr protein kinases. It is primarily expressed in neutrophils, myeloid-derived suppressor cells, macrophages, mast cells, and B lymphocytes but can also be expressed in nonimmune cells.[42] Its function in solid tumors is not entirely clear, with a possible tumor suppressive function.[43] In ES, an oncogenic signaling axis involving SYK, c-MYC, and MALAT1 has been described and may potentially serve as a therapeutic target.[44] Small-molecule inhibitors of SYK have shown antineoplastic properties and are currently explored in clinical trials for malignant and autoimmune diseases.[45]

As described in other *CIC*-rearranged sarcomas, in 3 of the CIC-rearranged sarcomas with *AXL, CITED1,* and *SYK* partners, there was ETV1 and ETV4 mRNA overexpression in keeping with strong transcriptional activation by CIC HMG box binding to the promoter of *PEA* genes.[11,12,46] By immunohistochemistry, all examined cases showed ETV4 positivity, albeit with variable expression, whereas WT1 was detected only in 1 of the 4 cases. However, there were 2 cases in which ETV4 immunohistochemical expression was only focal (<5% of tumor volume), and in 1 of them, WT1 showed negative results (WT1 not performed in the other). These findings may suggest a lower sensitivity for ETV4 and WT1 immunoexpression in tumors with rare *CIC* partners compared with *CIC::DUX4* sarcomas, in which it has been reported as 90% and 95%, respectively.[17]

One case in our cohort (case 5 with *CIC::SYK*) showed coexpression of CD31 and ERG and was initially diagnosed as epithelioid angiosarcoma. In 2017, Huang et al[11] reported 2 cases of epithelioid

angiosarcomas with diffuse expression of CD31/ERG and *CIC* rearrangements. They occurred in the kidney and soft tissues of adult female patients and histologically they were composed of solid round to epithelioid cells with no vasoformative features. *CIC::LEUTX* fusion was detected in 1 case in which the fusion partner was available, whereas concomitant *CIC* mutations were found in 2 cases. Recently, Kojima et al[47] reported 9 cases of *CIC*-rearranged sarcomas with coexpression of CD31 and ERG: 4 cases showed diffuse or strong expression of CD31, whereas none showed combined uniform diffuse and strong expression of both markers. Their clinicopathologic characteristics did not differ from the remaining 21 cases of their cohort. Three patients were initially diagnosed and treated as angiosarcoma with no clinical response. In contrast to conventional epithelioid angiosarcomas, these *CIC*-rearranged "angiosarcomas" did not exhibit vasoformative features and expressed ETV4 and/or WT1 immunohistochemically. Four cases examined by NGS did not harbor *CIC* missense mutations; by DNA methylation profiling a $CD31^+$ *CIC*-rearranged sarcoma clustered with $CD31^-$ *CIC*-rearranged sarcomas, distant from angiosarcomas. Unsupervised clustering of methylation profiles by t-SNE showed that the $CD31^+/ERG^+$ case in our cohort clustered tightly with the *CIC* sarcoma methylation class. These findings suggest that *CIC*-rearranged sarcomas with CD31/ERG coexpression likely belong to the *CIC*-rearranged URCS family rather than representing bone fide angiosarcomas. Moreover, 2 of the previously reported epithelioid angiosarcomas with *CIC* rearrangements showed overlapping gene signature with *CIC::DUX4* undifferentiated sarcomas by unsupervised hierarchical clustering, with significant overexpression of *ETV1/4/5* and *WT1* genes compared with a control group of conventional angiosarcomas.[11]

CIC-rearranged sarcomas have a distinct methylation profile.[22] Unsupervised clustering of methylation profiles by t-SNE showed that the 4 evaluated cases of our cohort clustered tightly together and along the *CIC* sarcoma methylation class. Intriguingly, rare cases of undifferentiated sarcomas (4 in the CNS and 1 of unknown origin) with *ATXN1::DUX4*, *ATXN1:NUTM2A*, and *ATXN1L-NUTM2A* fusions showed similar morphologic and immunohistochemical profile, *ETV1/4/5* upregulation and matched with the *CIC*-rearranged sarcomas by DNA methylation profile.[48-50] In less well-documented reports, 1 case with *ATXN1::NUTM1* and 1 with *CIC* frame-shift deletion along with a cell line with an in-frame *CIC* deletion also clustered with *CIC*-rearranged sarcomas.[46,48,51,52] The ATXN1/ATXN1L forms a transcriptional repressor complex with CIC, which represses its target genes by binding to DNA.[53] It is hypothesized that the *ATXN1/ATXN1L* fusions alter their protein structure and destabilize the protein complex with CIC, which leads to downstream gene overexpression and oncogenesis.[50] These recent data suggest that the categorization as "*CIC*-rearranged undifferentiated sarcoma" may be too restrictive to capture otherwise identical tumors and perhaps the term "undifferentiated sarcoma with upregulation of ETV1/4/5" may actually be more inclusive.

In conclusion, we report 5 cases of *CIC*-rearranged sarcomas with novel and rare partners. They were within the morphologic spectrum of URCSs, showed upregulation of ETV1 and ETV4, and were classified under *CIC*-rearranged sarcomas by unsupervised methylation clustering. This report expands the molecular diversity of this rare neoplasm.

Author Contributions

K.L. and C.R.A designed the study and interpreted clinicopathologic, immunohistochemical, and molecular data. J.K.D and T.B conducted the molecular analyses. J.L.H conducted the ETV4 immunohistochemical analyses. K.L wrote the manuscript with contributions from all other authors, who agreed on the final version.

Data Availability

All data used in this study are available and can be accessed on reasonable request.

Funding

This study was supported by P50 CA217694 (to C.R.A, W.T, S.S), P30 CA008748 (to C.R.A), Cycle for Survival (to C.R.A), and Kristin Ann Carr Foundation (to C.R.A)

Declaration of Competing Interest

The authors have no conflicts of interest to disclose.

Ethical Approval and Consent to Participate

Ethical approval was obtained for this study from the institutional review board of Memorial Sloan Kettering Cancer Center.

Supplementary Material

The online version contains supplementary material available at https://doi.org/10.1016/j.modpat.2023.100103.

References

1. Antonescu CR, Owosho AA, Zhang L, et al. Sarcomas with CIC-rearrangements are a distinct pathologic entity with aggressive outcome: a clinicopathologic and molecular study of 115 cases. *Am J Surg Pathol*. 2017;41(7):941–949.
2. Yoshimoto M, Graham C, Chilton-MacNeill S, et al. Detailed cytogenetic and array analysis of pediatric primitive sarcomas reveals a recurrent CIC-DUX4 fusion gene event. *Cancer Genet Cytogenet*. 2009;195(1):1–11.
3. Italiano A, Sung YS, Zhang L, et al. High prevalence of CIC fusion with double-homeobox (DUX4) transcription factors in EWSR1-negative undifferentiated small blue round cell sarcomas. *Genes Chromosomes Cancer*. 2012;51(3):207–218.
4. Yoshida A, Goto K, Kodaira M, et al. CIC-rearranged sarcomas: a study of 20 cases and comparisons with Ewing sarcomas. *Am J Surg Pathol*. 2016;40(3):313–323.
5. Sugita S, Arai Y, Aoyama T, et al. NUTM2A-CIC fusion small round cell sarcoma: a genetically distinct variant of CIC-rearranged sarcoma. *Hum Pathol*. 2017;65:225–230.
6. Sugita S, Arai Y, Tonooka A, et al. A novel CIC-FOXO4 gene fusion in undifferentiated small round cell sarcoma: a genetically distinct variant of Ewing-like sarcoma. *Am J Surg Pathol*. 2014;38(11):1571–1576.
7. Watson S, Perrin V, Guillemot D, et al. Transcriptomic definition of molecular subgroups of small round cell sarcomas. *J Pathol*. 2018;245(1):29–40.
8. Dissanayake K, Toth R, Blakey J, et al. ERK/p90(RSK)/14-3-3 signalling has an impact on expression of PEA3 Ets transcription factors via the transcriptional repressor capicua. *Biochem J*. 2011;433(3):515–525.
9. Astigarraga S, Grossman R, Diaz-Delfin J, Caelles C, Paroush Z, Jimenez G. A MAPK docking site is critical for downregulation of Capicua by Torso and EGFR RTK signaling. *EMBO J*. 2007;26(3):668–677.
10. Jimenez G, Guichet A, Ephrussi A, Casanova J. Relief of gene repression by torso RTK signaling: role of capicua in *Drosophila* terminal and dorsoventral patterning. *Genes Dev*. 2000;14(2):224–231.
11. Huang SC, Zhang L, Sung YS, et al. Recurrent CIC gene abnormalities in angiosarcomas: a molecular study of 120 cases with concurrent investigation of PLCG1, KDR, MYC, and FLT4 gene alterations. *Am J Surg Pathol*. 2016;40(5):645–655.

12. Kawamura-Saito M, Yamazaki Y, Kaneko K, et al. Fusion between CIC and DUX4 up-regulates PEA3 family genes in Ewing-like sarcomas with t(4;19)(q35;q13) translocation. *Hum Mol Genet*. 2006;15(13):2125–2137.
13. Specht K, Sung YS, Zhang L, Richter GH, Fletcher CD, Antonescu CR. Distinct transcriptional signature and immunoprofile of CIC-DUX4 fusion-positive round cell tumors compared to EWSR1-rearranged Ewing sarcomas: further evidence toward distinct pathologic entities. *Genes Chromosomes Cancer*. 2014;53(7):622–633.
14. Oh S, Shin S, Janknecht R. ETV1, 4 and 5: an oncogenic subfamily of ETS transcription factors. *Biochim Biophys Acta*. 2012;1826(1):1–12.
15. Kao YC, Sung YS, Chen CL, et al. ETV transcriptional upregulation is more reliable than RNA sequencing algorithms and FISH in diagnosing round cell sarcomas with CIC gene rearrangements. *Genes Chromosomes Cancer*. 2017;56(6):501–510.
16. Yoshida A, Arai Y, Kobayashi E, et al. CIC break-apart fluorescence in-situ hybridization misses a subset of CIC-DUX4 sarcomas: a clinicopathological and molecular study. *Histopathology*. 2017;71(3):461–469.
17. Hung YP, Fletcher CD, Hornick JL. Evaluation of ETV4 and WT1 expression in CIC-rearranged sarcomas and histologic mimics. *Mod Pathol*. 2016;29(11):1324–1334.
18. Smith SC, Palanisamy N, Martin E, et al. The utility of ETV1, ETV4 and ETV5 RNA in-situ hybridization in the diagnosis of CIC-DUX sarcomas. *Histopathology*. 2017;70(4):657–663.
19. Zhu G, Benayed R, Ho C, et al. Diagnosis of known sarcoma fusions and novel fusion partners by targeted RNA sequencing with identification of a recurrent ACTB-FOSB fusion in pseudomyogenic hemangioendothelioma. *Mod Pathol*. 2019;32(5):609–620.
20. Zehir A, Benayed R, Shah RH, et al. Mutational landscape of metastatic cancer revealed from prospective clinical sequencing of 10,000 patients. *Nat Med*. 2017;23(6):703–713.
21. Benhamida JK, Hechtman JF, Nafa K, et al. Reliable clinical MLH1 promoter hypermethylation assessment using a high-throughput genome-wide methylation array platform. *J Mol Diagn*. 2020;22(3):368–375.
22. Koelsche C, Schrimpf D, Stichel D, et al. Sarcoma classification by DNA methylation profiling. *Nat Commun*. 2021;12(1):498.
23. Aryee MJ, Jaffe AE, Corrada-Bravo H, et al. Minfi: a flexible and comprehensive Bioconductor package for the analysis of Infinium DNA methylation microarrays. *Bioinformatics*. 2014;30(10):1363–1369.
24. Du P, Zhang X, Huang CC, et al. Comparison of beta-value and M-value methods for quantifying methylation levels by microarray analysis. *BMC Bioinformatics*. 2010;11:587.
25. Niu B, Ye K, Zhang Q, et al. MSIsensor: microsatellite instability detection using paired tumor-normal sequence data. *Bioinformatics*. 2014;30(7):1015–1016.
26. Solomon DA, Brohl AS, Khan J, Miettinen M. Clinicopathologic features of a second patient with Ewing-like sarcoma harboring CIC-FOXO4 gene fusion. *Am J Surg Pathol*. 2014;38(12):1724–1725.
27. Le Loarer F, Pissaloux D, Watson S, et al. Clinicopathologic features of CIC-NUTM1 sarcomas, a new molecular variant of the family of CIC-fused sarcomas. *Am J Surg Pathol*. 2019;43(2):268–276.
28. Yang S, Liu L, Yan Y, et al. CIC-NUTM1 sarcomas affecting the spine. *Arch Pathol Lab Med*. 2022;146(6):735–741.
29. Smith SC, Buehler D, Choi EY, et al. CIC-DUX sarcomas demonstrate frequent MYC amplification and ETS-family transcription factor expression. *Mod Pathol*. 2015;28(1):57–68.
30. Linger RM, Keating AK, Earp HS, Graham DK. TAM receptor tyrosine kinases: biologic functions, signaling, and potential therapeutic targeting in human cancer. *Adv Cancer Res*. 2008;100:35–83.
31. Karanian M, Kelsey A, Paindavoine S, et al. SRF fusions other than with RELA expand the molecular definition of SRF-fused perivascular tumors. *Am J Surg Pathol*. 2020;44(12):1725–1735.
32. Alaggio R, Zhang L, Sung YS, et al. A molecular study of pediatric spindle and sclerosing rhabdomyosarcoma: identification of novel and recurrent VGLL2-related fusions in infantile cases. *Am J Surg Pathol*. 2016;40(2):224–235.
33. Puls F, Carter JM, Pillay N, et al. Overlapping morphological, immunohistochemical and genetic features of superficial CD34-positive fibroblastic tumor and PRDM10-rearranged soft tissue tumor. *Mod Pathol*. 2022;35(6):767–776.
34. Kumar-Sinha C, Anderson B, Heider A, et al. Clinical sequencing of high-grade undifferentiated sarcomas: a case series and report of an aggressive primary cardiac tumor with multiple oncogenic drivers. *JCO Precis Oncol*. 2020;4.PO.19.00322.
35. Holland PW, Booth HA, Bruford EA. Classification and nomenclature of all human homeobox genes. *BMC Biol*. 2007;5:47.
36. Song K, Huang Y, Xia CD, Zhu HQ, Wang J. A case of CIC-rearranged sarcoma with CIC-LEUTX gene fusion in spinal cord. *Neuropathology*. 2022;42(6):555–562.
37. Barresi S, Giovannoni I, Rossi S, et al. A novel BRD4-LEUTX fusion in a pediatric sarcoma with epithelioid morphology and diffuse S100 expression. *Genes Chromosomes Cancer*. 2021;60(9):647–652.
38. Chinen Y, Taki T, Tsutsumi Y, et al. The leucine twenty homeobox (LEUTX) gene, which lacks a histone acetyltransferase domain, is fused to KAT6A in therapy-related acute myeloid leukemia with t(8;19)(p11;q13). *Genes Chromosomes Cancer*. 2014;53(4):299–308.
39. Hu W, Wang J, Yuan L, et al. Case report: a unique case of pediatric central nervous system embryonal tumor harboring the CIC-LEUTX fusion, germline NBN variant and somatic TSC2 mutation: expanding the spectrum of CIC-rearranged neoplasia. *Front Oncol*. 2020;10:598970.
40. Lake JA, Donson AM, Prince E, et al. Targeted fusion analysis can aid in the classification and treatment of pediatric glioma, ependymoma, and glioneuronal tumors. *Pediatr Blood Cancer*. 2020;67(1):e28028.
41. Noch ENB, Chan J, Wolden S, Tap W, Antonescu C, Khakoo Y. A 43 year-old woman with primary central nervous system angiosarcoma with CIC-LEUTX gene rearrangement. *Neurology*. 2019;92. P3.6–017.
42. Aguirre-Ducler A, Gianino N, Villarroel-Espindola F, et al. Tumor cell SYK expression modulates the tumor immune microenvironment composition in human cancer via TNF-alpha dependent signaling. *J Immunother Cancer*. 2022;10(7):e005113.
43. Bailet O, Fenouille N, Abbe P, et al. Spleen tyrosine kinase functions as a tumor suppressor in melanoma cells by inducing senescence-like growth arrest. *Cancer Res*. 2009;69(7):2748–2756.
44. Sun H, Lin DC, Cao Q, et al. Identification of a novel SYK/c-MYC/MALAT1 signaling pathway and its potential therapeutic value in Ewing sarcoma. *Clin Cancer Res*. 2017;23(15):4376–4387.
45. Sharman J, Hawkins M, Kolibaba K, et al. An open-label phase 2 trial of entospletinib (GS-9973), a selective spleen tyrosine kinase inhibitor, in chronic lymphocytic leukemia. *Blood*. 2015;125(15):2336–2343.
46. Sturm D, Orr BA, Toprak UH, et al. New brain tumor entities emerge from molecular classification of CNS-PNETs. *Cell*. 2016;164(5):1060–1072.
47. Kojima N, Arai Y, Satomi K, et al. Co-expression of ERG and CD31 in a subset of CIC-rearranged sarcoma: a potential diagnostic pitfall. *Mod Pathol*. 2022;35(10):1439–1448.
48. Pratt D, Kumar-Sinha C, Cieslik M, et al. A novel ATXN1-DUX4 fusion expands the spectrum of 'CIC-rearranged sarcoma' of the CNS to include non-CIC alterations. *Acta Neuropathol*. 2021;141(4):619–622.
49. Satomi K, Ohno M, Kubo T, et al. Central nervous system sarcoma with ATXN1::DUX4 fusion expands the concept of CIC-rearranged sarcoma. *Genes Chromosomes Cancer*. 2022;61(11):683–688.
50. Xu F, Viaene AN, Ruiz J, et al. Novel ATXN1/ATXN1L::NUTM2A fusions identified in aggressive infant sarcomas with gene expression and methylation patterns similar to CIC-rearranged sarcoma. *Acta Neuropathol Commun*. 2022;10(1):102.
51. Siegfried A, Masliah-Planchon J, Roux FE, et al. Brain tumor with an ATXN1-NUTM1 fusion gene expands the histologic spectrum of NUTM1-rearranged neoplasia. *Acta Neuropathol Commun*. 2019;7(1):220.
52. Fults D, Pedone CA, Morse HG, Rose JW, McKay RD. Establishment and characterization of a human primitive neuroectodermal tumor cell line from the cerebral hemisphere. *J Neuropathol Exp Neurol*. 1992;51(3):272–280.
53. Lu HC, Tan Q, Rousseaux MW, et al. Disruption of the ATXN1-CIC complex causes a spectrum of neurobehavioral phenotypes in mice and humans. *Nat Genet*. 2017;49(4):527–536.